Supplementary Information for:

An All-rounder Aminoguanidine based Ligand, Its Unusual Anionic Zinc(II) and Cadmium(II) Coordination Complexes and Their Biological Implications

Ansa Santu[a], K. K. Mohammed Hashim[a], E. Manoj[a*]

[a]*Department of Applied Chemistry, CUSAT, Kochi, Kerala 682 022, India*
*manoje@cusat.ac.in

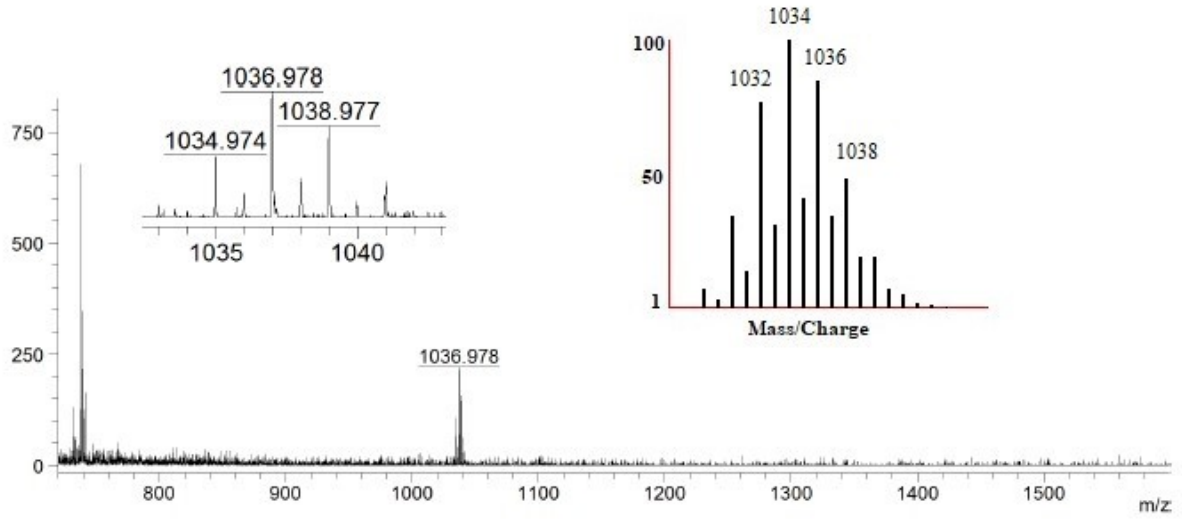

Figure S1. Mass spectrum of $[ZnCl_2(H_4Brsal\text{-}dag)]H_6Brsal\text{-}dag.DMF.H_2O$ with experimental and calculated isotopic patterns.

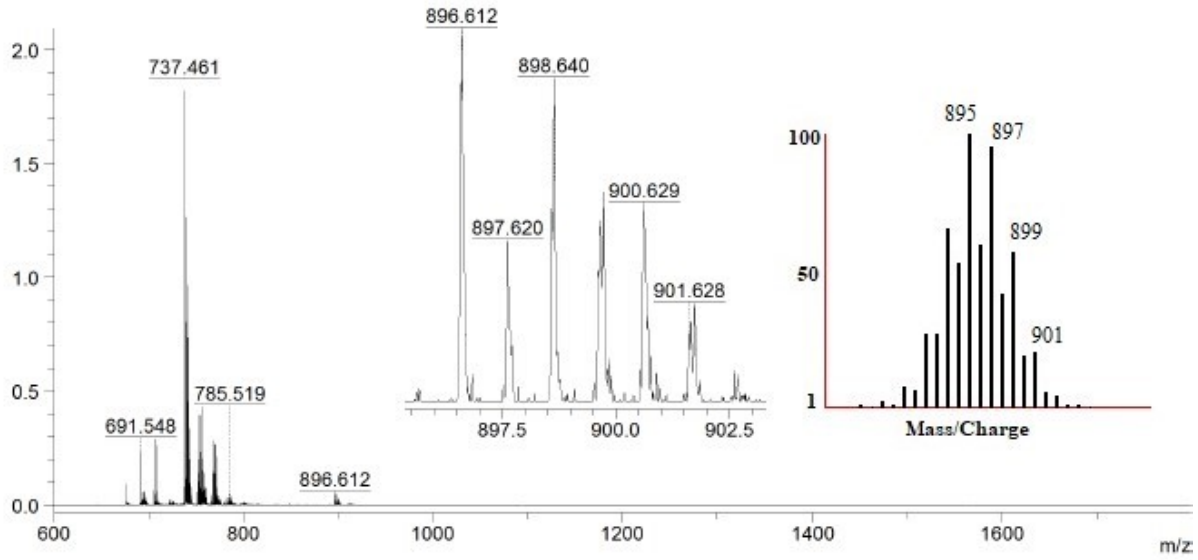

Figure S2. Mass spectrum of $[CdCl_2(H_4Brsal\text{-}dag)]H_6Brsal\text{-}dag.DMF.H_2O$ with experimental and calculated isotopic patterns.

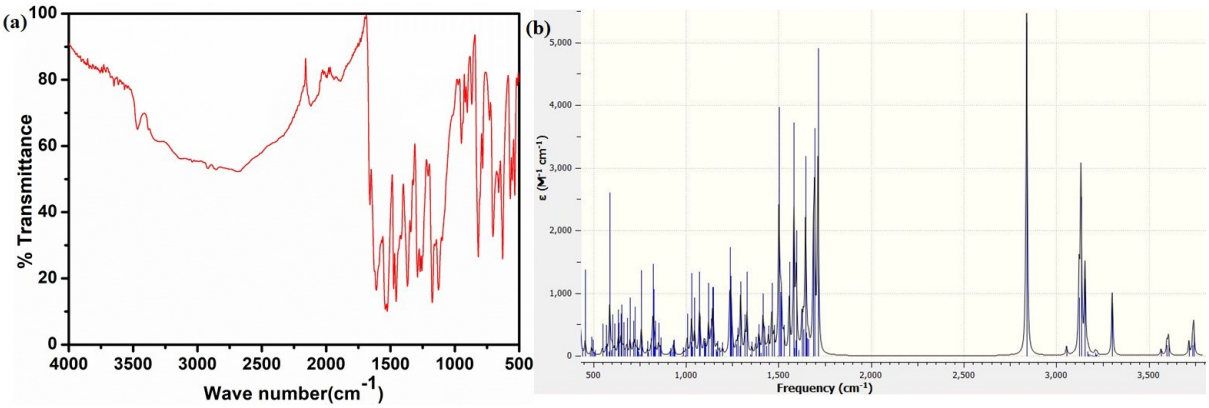

Figure S3. Experimental (a) and theoretical (b) IR spectra of the complex **1**.

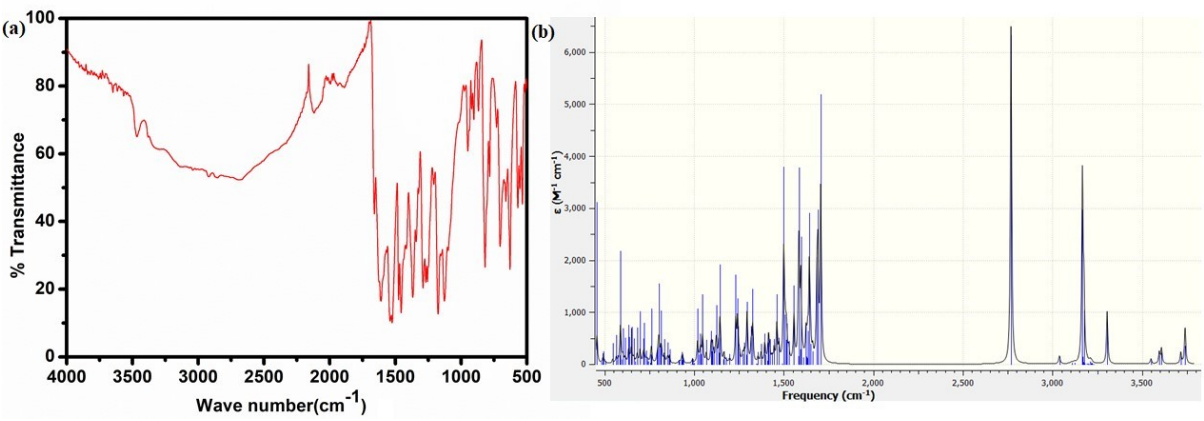

Figure S4. Experimental (a) and theoretical (b) IR spectra of the complex **2**.

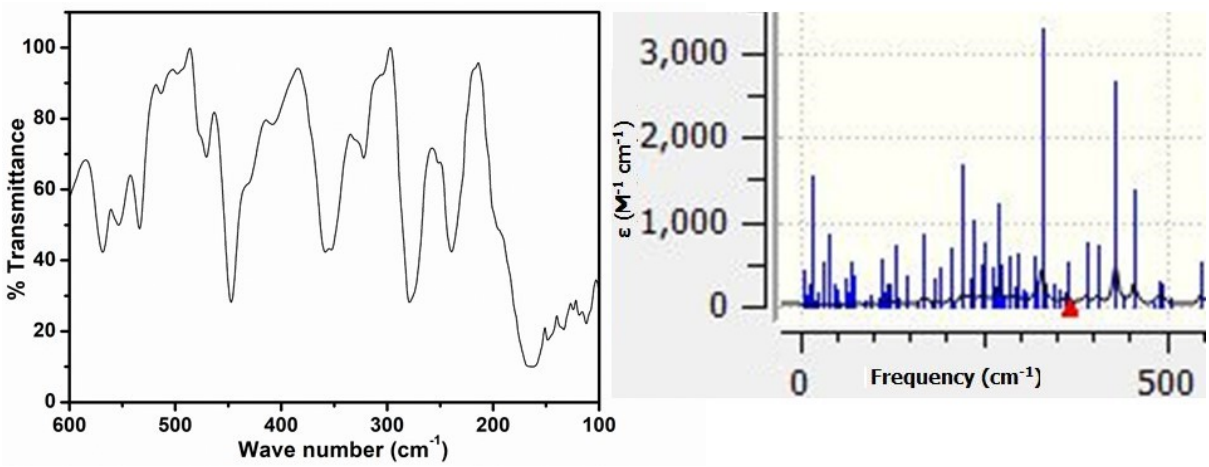

Figure S5. Experimental (a) and theoretical (b) Far IR spectra of the complex **1.**

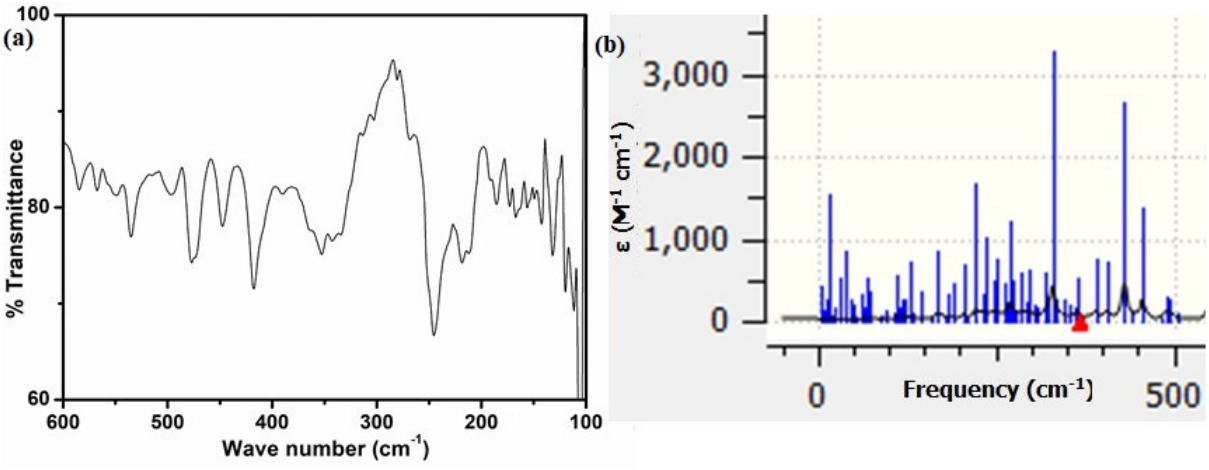

Figure S6. Experimental (a) and theoretical (b) Far IR spectra of the complex **2**.

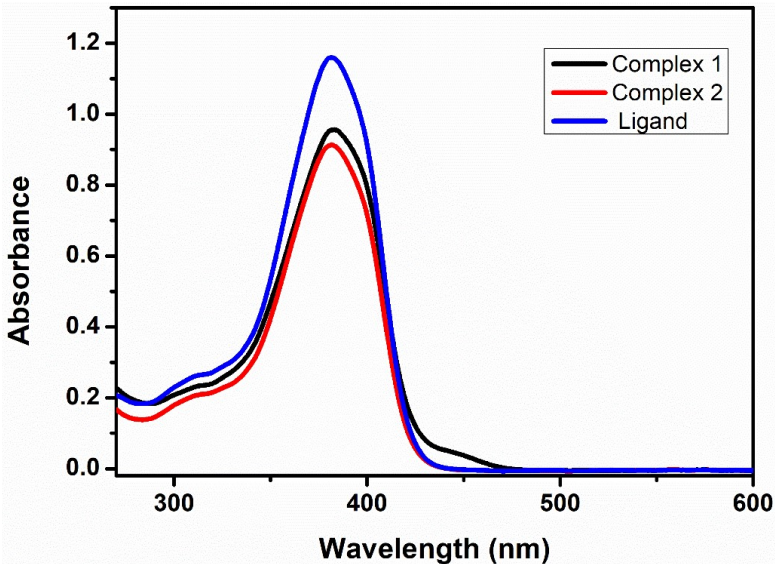

Figure S7. UV-vis spectra of the ligand, complex **1** and complex **2**.

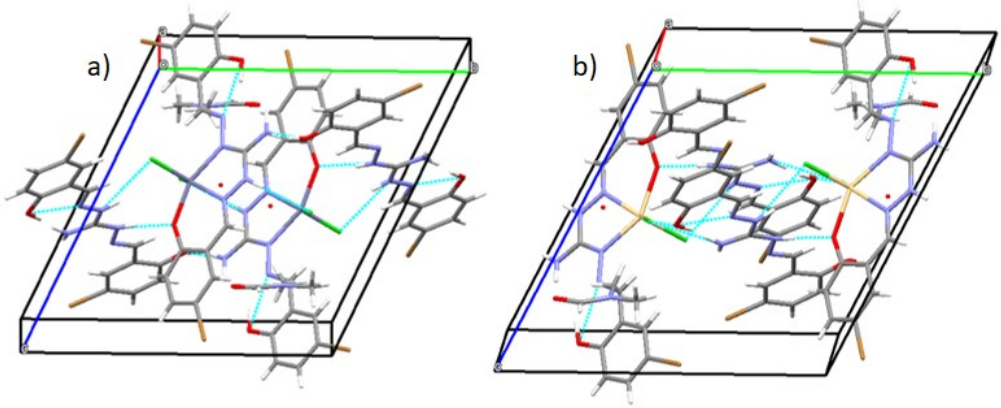

Figure S8. Unit cell packing diagrams of a) complex **1** and b) complex **2** along the 'a' axis, showing relevant hydrogen bonding interactions (blue dotted lines).

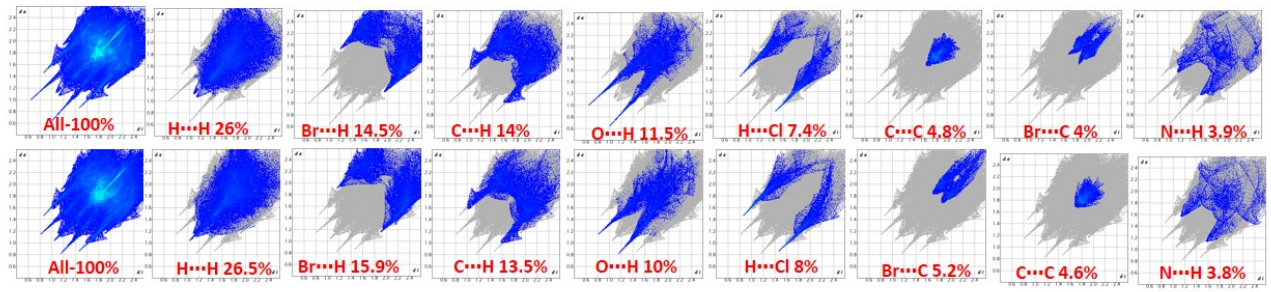

Figure S9. 2D Fingerprint plots showing the percentages of contacts contributed to the total Hirshfeld surface area of the complex **1**(below) and the complex **2** (above).

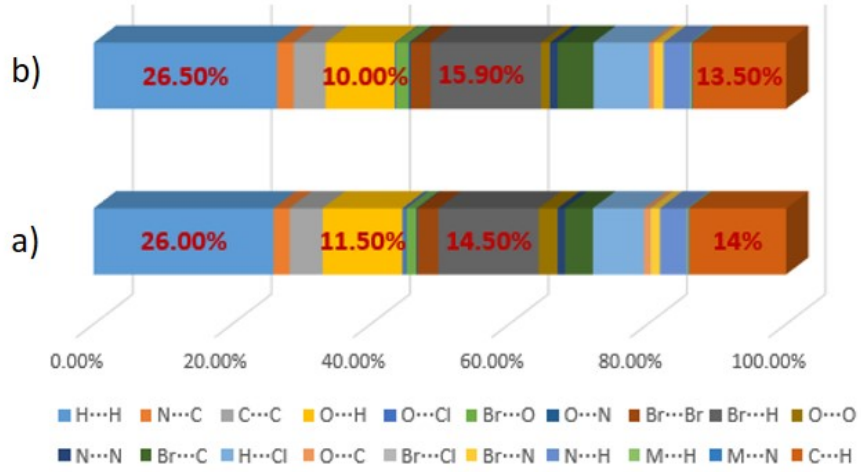

Figure S10. Relative contributions of various intermolecular contacts to the Hirshfeld surface area in a) complex **1** and b) complex **2.**

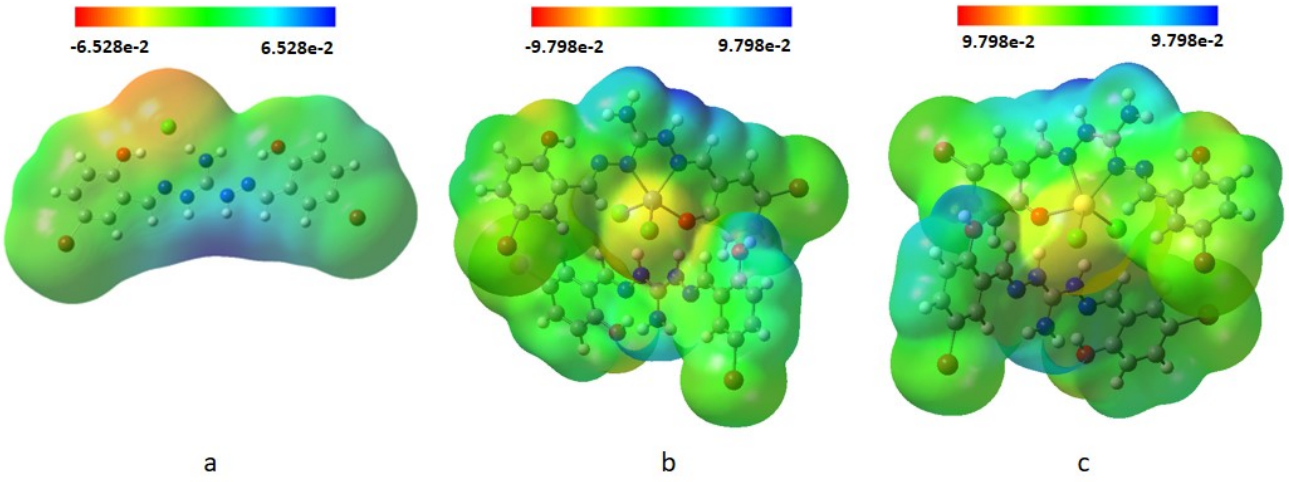

Figure S11. MEP plots for (a) ligand, (b) complex **1** and (c) complex **2**.

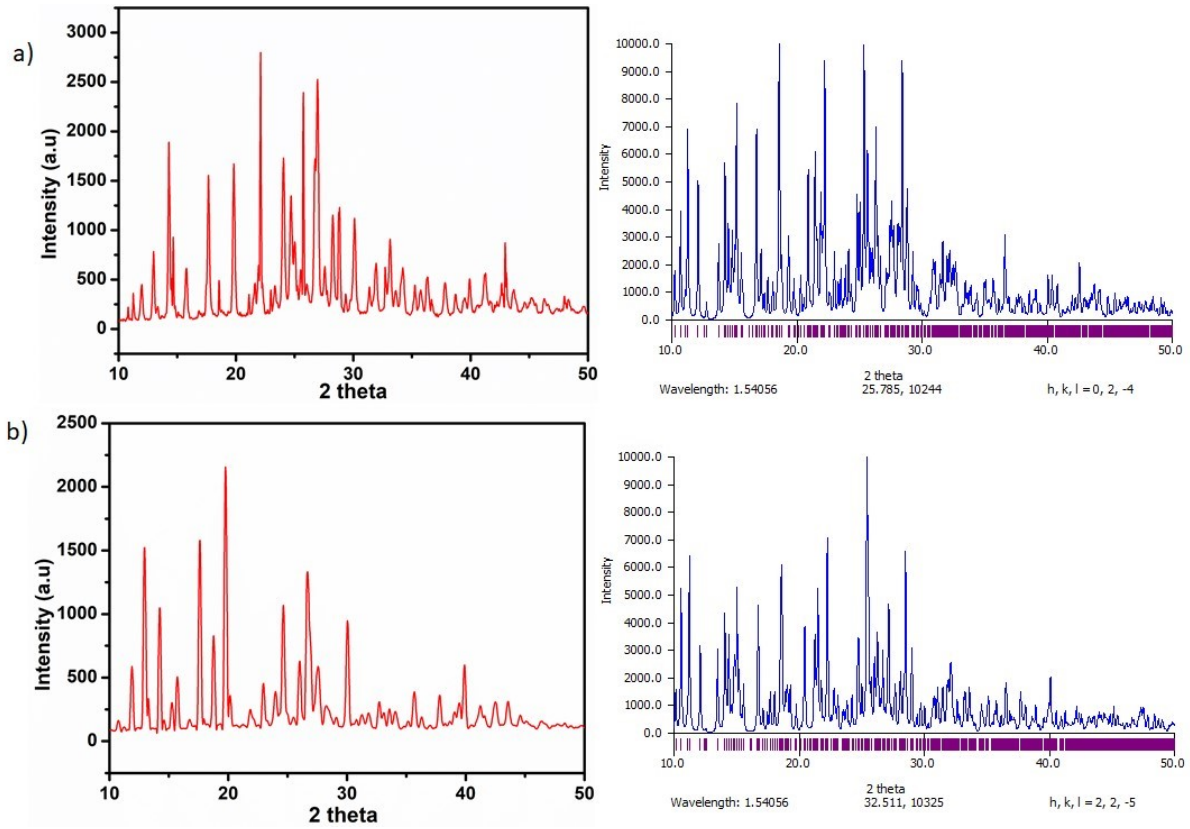

Figure S12. PXRD (left) and simulated PXRD pattern from SC-XRD (right) of (a) the complex **1** and (b) the complex **2**.

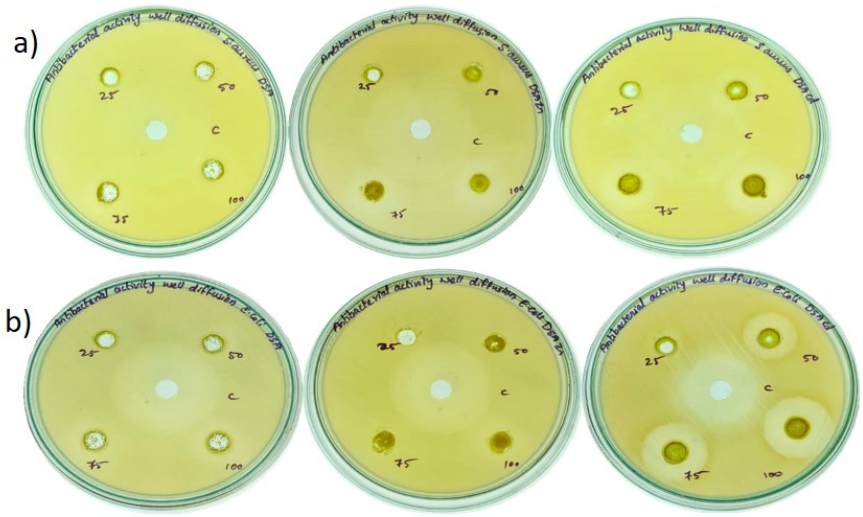

Figure S13. Zone of inhibition of (a) *S.aureus* (b) *E.coli* against ligand, complex **1** and complex **2.**

.

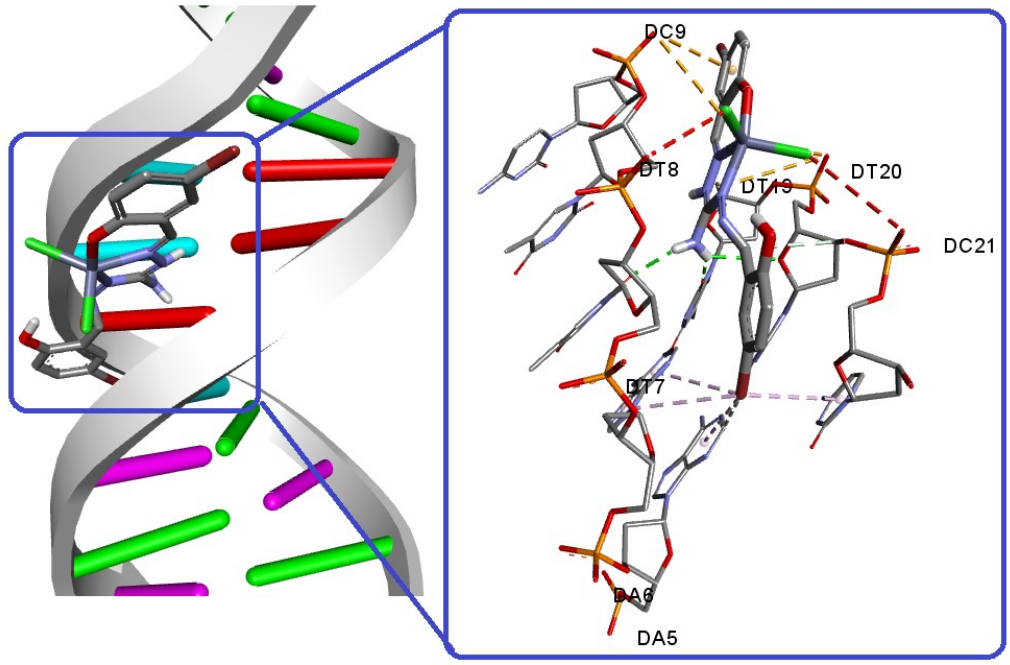

Figure S14. Binding mode of $[ZnCl_2(H_4Brsal\text{-}dag)]^-$ and its focused view of interactions with 1BNA.

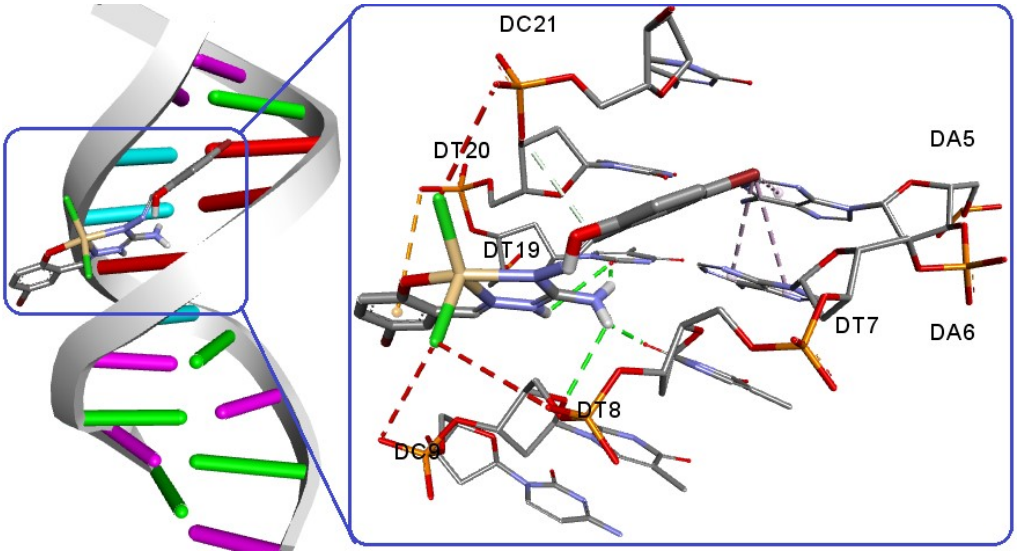

Figure S15. Binding mode of $[CdCl_2(H_4Brsal\text{-}dag)]^-$ and its focused view of interactions with 1BNA.

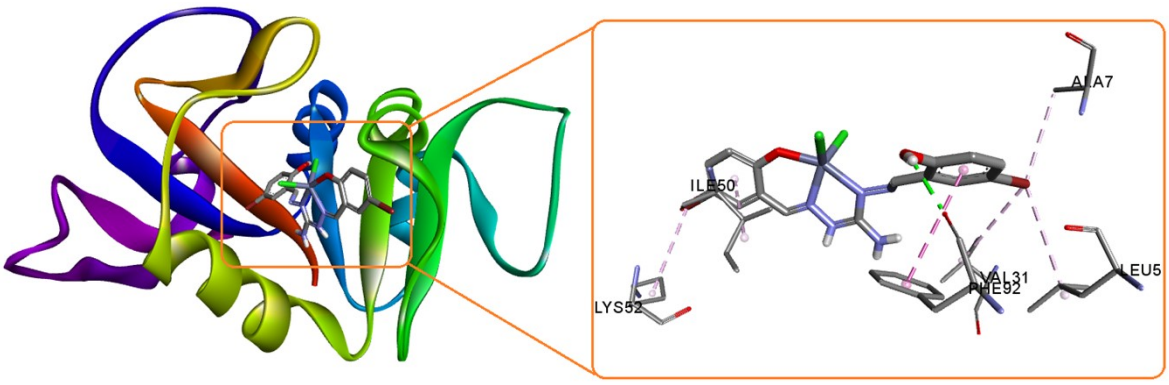

Figure S16. Binding mode of $[ZnCl_2(H_4Brsal\text{-}dag)]^-$ and its focused view of interactions with DHFR from *S. aureus*.

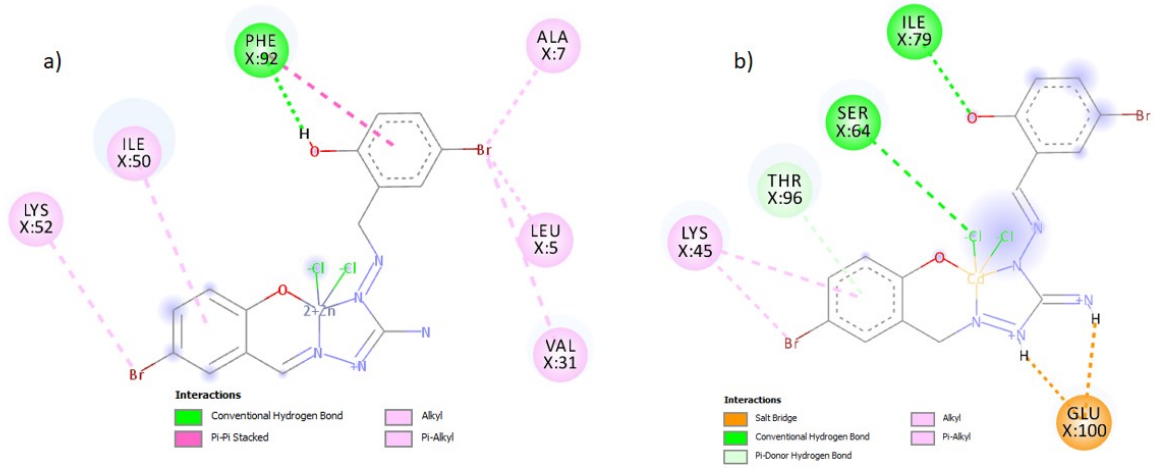

Figure S17. 2D representation of (a) $[ZnCl_2(H_4Brsal\text{-}dag)]^-$ and (b) $[CdCl_2(H_4Brsal\text{-}dag)]^-$ at the active site residues of DHFR from *S. aureus*.

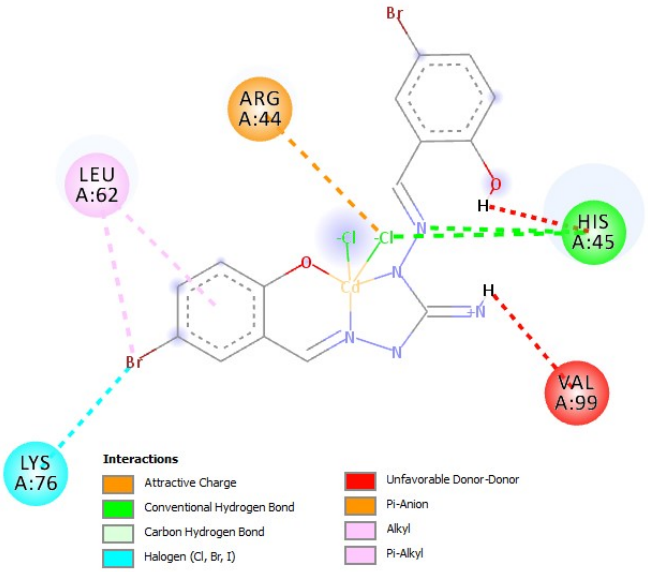

Figure S18. 2D representation of $[CdCl_2(H_4Brsal\text{-}dag)]^-$ with the active site residues of DHFR from *E. coli*.

Table S1. Crystal refinement parameters of the complexes $[ZnCl_2(H_4Brsal\text{-}dag)]H_6Brsal\text{-}dag\cdot DMF\cdot H_2O$ (**1**) and $[CdCl_2(H_4Brsal\text{-}dag)]H_6Brsal\text{-}dag\cdot DMF\cdot H_2O$ (**2**).

Parameters	$[ZnCl_2(H_4Brsal\text{-}dag)]H_6Brsal\text{-}dag\cdot DMF\cdot H_2O$	$[CdCl_2(H_4Brsal\text{-}dag)]H_6Brsal\text{-}dag\cdot DMF\cdot H_2O$
CCDC number	2259210	2290289
Empirical Formula	$C_{33}H_{35}Br_4Cl_2N_{11}O_6Zn$	$C_{33}H_{35}Br_4CdCl_2N_{11}O_6$
Formula weight (M)	1137.63	1184.66
Temperature (T)	295(2) K	298(2) K
Wavelength (Mo/Cu Kα)	1.54178 Å	0.71073 Å
Crystal system	triclinic	triclinic
Space group	*P-1*	*P-1*
Unit cell dimensions	a=12.4293(3)Å α=115.0430(10)° b = 13.9253(3)Å β= 99.3430(10)° c= 14.0492(3)Å γ= 95.0030(10)°	a =12.3459(7) Å α=116.555(2)° b =14.1549(9) Å β=99.070(2)° c= 14.4164(9) Å γ=94.806(2)°
Volume V, Z	2140.51(8) $Å^3$, 2	2191.2(2) $Å^3$, 2
Calculated density (ρ)	1.765 g/cm^3	1.796 g/cm^3
Absorption coefficient, μ	6.792 mm^{-1}	4.322 mm^{-1}
F(000)	1124	1160
Crystal size	0.223 x 0.052 x 0.035 mm	0.305 x 0.196 x 0.124 mm
Limiting Indices	-14≤h≤14, -16≤k<=15, -16≤l<=16	-15≤h≤15, -17≤k<=17, -17≤l<=17
Reflections collected	77726	100702
Independent Reflections	7857[R(int) =0.1049]	8307[R(int) =0.0623]
Refinement method	Full-matrix least-squares on F^2	Full-matrix least-squares on F^2
Data / restraints / parameters	7857/8/555	8307/10/554
Goodness-of-fit on F^2	1.065	1.084
Final *R* indices [I > 2σ (I)]	R_1 = 0.0510, wR_2 = 0.1046	R_1 = 0.0424, wR_2 = 0.0990
R indices (all data)	R_1 = 0.1142, wR_2 = 0.1250	R_1 = 0.0700, wR_2 = 0.1182
Weighing Scheme	'w=1/[\s^2^(Fo^2^)+(0.0432P)^2^ +4.6321P], where P=(Fo^2^+2Fc^2^)/3'	'w=1/[\s^2^(Fo^2^)+(0.0442P)^2^ +5.7744P], where P=(Fo^2^+2Fc^2^)/3'
Largest difference peak and hole	0.725 and -0.705 e $Å^{-3}$	0.925 and -1.111 e $Å^{-3}$

$R_1 = \Sigma||F_o| - |F_c|| / \Sigma|F_o|$; $wR_2 = [\Sigma w(F_o^2-F_c^2)^2 / \Sigma w(F_o^2)^2]^{1/2}$

Table S2. The bond lengths (Å) and bond angles (˚) of the complex [$CdCl_2$(H_4Brsal-dag)]H_6Brsal-dag.DMF.H_2O **(2)**.

Bond lengths (Å)		Bond angles (˚)	
Cd1–O1	2.216(3)	O1–Cd1–N1	79.12(14)
Cd1–N4	2.287(4)	O1–Cd1–N4	148.74(13)
Cd1–N1	2.327(4)	N1–Cd1–N4	70.86(15)
Cd1–Cl1	2.4861(13)	O1–Cd1–Cl1	98.22(10)
Cd1–Cl2	2.4884(13)	N1–Cd1–Cl1	111.96(11)
N4–N5	1.390(6)	N4–Cd1–Cl1	100.82(11)
C8–N3	1.314(6)	O1–Cd1–Cl2	91.84(10)
C8–N4	1.336(7)	N1–Cd1–Cl2	137.33(11)
N3–C8	1.355(7)	N4–Cd1–Cl2	104.22(11)
N1–N2	1.379(6)	Cl1–Cd1–Cl2	110.59(4)
N1–C7	1.283(7)		
O1–C1	1.326(6)		
O2–C15	1.354(7)		
Br2–C12	1.904(6)		
C4–Br1	1.914(5)		

Table S3. Interaction parameters of the complex $[CdCl_2(H_4Brsal\text{-}dag)]H_6Brsal\text{-}dag.DMF.H_2O$ **(2)**.

Hydrogen bonding interactions				
D–H ··· A	D–H (Å)	H ··· A (Å)	D--A (Å)	D–H ··· A (°)
N8–H8NB ··· N6	0.83(4)	2.45(4)	2.736(6)	101(3)
N8–H8NB ··· Cl(2)[a]	0.83(4)	2.49(4)	3.267(5)	156(3)
N8–H8NA ··· N10	0.84(3)	2.31(6)	2.667(7)	106(5)
N8–H8NA ··· Cl(1)[a]	0.84(3)	2.66(4)	3.370(5)	143(5)
N2–H2N ··· Cl(2)[b]	0.83(6)	2.63(3)	3.357(6)	147(6)
N2–H2N ··· O(6)[b]	0.83(6)	2.51(8)	3.135(15)	132(6)
O2–H20 ··· N5	0.96(5)	1.94(5)	2.714(6)	136(6)
N3–H3NA ··· O(3)[b]	0.84(6)	2.12(6)	2.906(9)	156(6)
O3–H30 ··· O(5)	0.95(8)	1.74(9)	2.627(13)	154(7)
N3–H3NB ··· N5	0.84(5)	2.30(8)	2.639(8)	104(6)
O4–H40 ··· N6	0.96(7)	1.94(8)	2.755(7)	141(6)
N7–H7N ··· Cl(1)	0.84(6)	2.44(5)	3.226(4)	157(5)
N9–H9N ··· O(1)	0.83(5)	1.86(5)	2.683(7)	175(5)
C9–H9 ··· Cl2	0.93	2.75	3.591(5)	150
C22–H22 ··· O3	0.93	2.45	2.767(8)	100
C32–H32A ··· O5	0.96	2.37	2.81(3)	108
D = donor, A = acceptor, Equivalent position codes a = 1-x,1-y,1-z; b =1- x,2-y,1-z;				

π ··· π interactions			
Cg ··· Cg	Cgv ··· Cg (Å)	α (°)	β (°)
Cg(1) ··· Cg(1)[a]	3.597(3)	0.0(2)	15.6
Cg(1) ··· Cg(2)[a]	3.784(3)	6.11(19)	28.7
Cg(2) ··· Cg(1)[a]	3.784(3)	6.11(19)	22.6
Cg(4) ··· Cg(4)[b]	3.895(4)	0.0(3)	26.8
Cg(5) ··· Cg(6)[c]	3.667(3)	9.3(3)	11.3
Cg(6) ··· Cg(5)[c]	3.667(3)	9.3(3)	20.2
Equivalent position codes: a= 1-x,2-y,1-z ;b= 1-x,1-y,-z ; c= 1-x,1`-y,1-z			

C–X ··· π interactions			
C–X ··· Cg	X ··· Cg (Å)	C ··· Cg (Å)	C-X ··· Cg (°)
C28–H28 ··· Cg(3)[a]	2.60	3.501(7)	163
Equivalent position codes: a= -x,1-y,1-z; Cg(3)= C(1), C(2), C(3), C(4), C(5), C(6).			

Table S4. The Frontier molecular orbital energies and calculated chemical reactivity parameters for the compounds.

Energy parameters (eV)	H_5Brsal-dag.HCl	Complex **1**	Complex **2**
HOMO	-5.93	-5.92	-5.93
HOMO-1	-6.21	-6.11	-6.61
LUMO	-3.02	-2.47	-2.48
LUMO+1	-2.16	-2.32	-2.29
E_{HOMO}–E_{LUMO}: ΔE	2.90	3.45	3.45
Ionization Energy, I	5.93	5.92	5.93
Electron Affinity, A	3.02	2.47	2.48
Chemical hardness, η	1.45	1.72	1.72
Electronegativity, χ	4.47	4.19	4.20
Chemical potential, μ	-4.47	-4.19	-4.20
Electrophilicity, ω	6.90	5.10	5.12
Total Energy	-4896645.56	-361630.84	-361153.39
Global softness, σ (eV^{-1})	0.68	0.58	0.68
Nucleophilicity,ε (eV^{-1})	0.14	0.19	0.19
Dipole moment (Debye)	12.94	8.24	8.17

Table S5. Results of the inhibitory zones and the % antimicrobial activity of the complexes**.**

Bacterial strains	Conc.(μL)	Complex **1**	Complex **2**	Ciprofloxacin
E.coli	25	-	11mm, (52.3%)	21mm, (100%)
	50	-	20mm, (95.23%)	
	75	-	24mm, (114.28%)	
	100	-	25mm, (119.04%)	
S.aureus	25	-	-	40mm, (100%)
	50	-	12mm, (30%)	
	75	10mm, (25%)	12mm, (30%)	
	100	11mm, (27.5%)	13mm, (32.5%)	